Improving SLM additive manufacturing operation precision with H-infinity controller structure

Fetra Rasoanarivo, Didier Dumur, Pedro Rodriguez-Ayerbe

Contents lists available at ScienceDirect

CIRP Journal of Manufacturing Science and Technology

Journal homepage: www.elsevier.com/locate/cirpj

Improving SLM additive manufacturing operation precision with H-infinity controller structure.

Fetra Rasoanarivo[a], Didier Dumur[a,*], Pedro Rodriguez-Ayerbe[a]

[a] *Université Paris-Saclay, CNRS, CentraleSupélec, Laboratoire des signaux et systèmes, 91190, Gif-sur-Yvette, France.*

Abstract

SLM (Selective Laser Melting) is the most widespread additive manufacturing technique of metal part. The desired part is elaborated through local melting of a raw metal powder bed by means of laser. In industrial machines, galvanometer motors achieve the laser beam deflection and focus control tasks. This paper proposes a H-infinity controller synthesis which improves the system accuracy and robustness towards physical features. Compared to a conventional control scheme, results obtained with the H-infinity controller implemented in an open architecture test bench consisting of a 2-axis laser deflection system showed improved accuracy performance while operation rapidity is optimized.

Keywords: Control, Modelling, Additive Manufacturing, Galvanometer, H-infinity control

Introduction

Selective Laser Melting (SLM, also referred to as LBM: Laser Beam Melting) is the most common process for Additive Manufacturing (AM) of metal parts in modern industrial machines. Current performances of AM machines enabled AM processes for production of small series with the attendant technological challenges constantly growing in both industry and academia [1]. The performance of the SLM process chain hinges on five major points of interest [2]: *'Equipment'*, *'Material'*, *'Production'*, *'Batch'*, *'Part Finishing'*. Certain physical aspects of metal powder melting remain lesser known, and a current research trend is oriented towards modelling these physical phenomena [3]. The work presented in this paper deals with the mechanical actuators control of the production machine.

In the '*Equipment*' category, the main actuator element for SLM machines is the three-axis deflection and focus control system (Figure 1). The control strategy of the galvanometer motor which drives each axis of the actuator is addressed here.

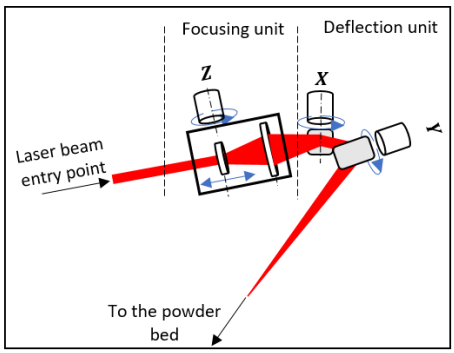

Figure 1. Three-axis actuator for SLM machines.

The galvanometer motor is mostly used in a closed-loop control framework [4]. The controller structure is synthetized so as to meet the precision and rapidity requirements of the operation. Control strategies of the galvanometer motor have been extensively studied in the automatic control field, as an example of high precision system. The reference [5] proposes a general framework in which the synthesis of the controller can be divided into four main points of interest towards the improvement of the closed-loop dynamics: '*Feedforward/ Command Shaping*', '*Feedback Control*', '*Modeling/Identification*' and '*Optimization/ Auto tuning*'. The most-encountered conventional structures in industry are Proportional-Integral-Derivative (PID)-based controllers [4]. State of the art works supply a large panel of advanced controller schemes that tackle specific problems such as residual vibration suppression by initial value compensation techniques [6], disturbance rejection through enhancement of the controller with an observer [7] or online closed-loop dynamics enhancement with adaptive control strategies [8].

In this paper, we propose an H-infinity robust controller [9] structure synthesis based on the desired closed-loop behavior of the galvanometer system. Compared to the dynamics enhancement techniques mentioned above, the H-infinity controller synthesis takes into account multiple synthesis objectives all at once (stability, rapidity, precision and torsional bending modes rejection). Moreover, H-infinity robust controllers have already been extensively used in industry for mechanical servo systems [10]. Performance achieved with actuator axes driven with PID-based conventional structures and the newly introduced H-infinity structures are compared in this work within the framework of an experimental marking job. It is shown that the operation precision is improved with H-infinity structures driving the actuator axes when operation rapidity is optimized. An open architecture test bench is developed with a conventional control structure, following the H-infinity synthesis technique is applied to the control of galvanometers.

The open-architecture test bench

Experiments are carried out on a 2-axis open architecture test bench as presented in Figure 2. The setup, designed to reproduce the real behavior of a commercial system, consists of a 2-axis

* Corresponding author.
E-mail address: didier.dumur@centralesupelec.fr (D. Dumur)

commercial galvanometer scanner system (motor and mirror) along with its control card. The addition of an external control card allows for an open-architecture framework, providing implementation of proposed control structures. Developed control strategies are implemented in Matlab/Simulink® in a PC workstation connected to the test bench by means of a dSpace interface board.

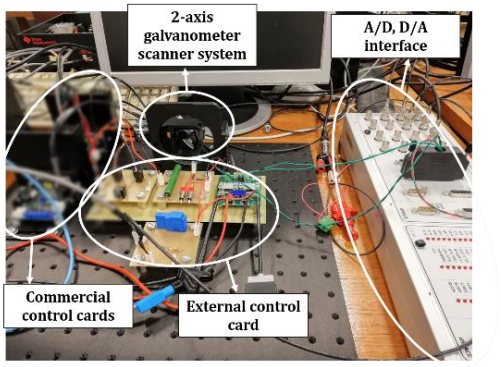

Figure 2. Open-architecture galvanometer test bench.

For the SLM process of additive manufacturing, limited speed variations are inherent to the technique. In fact, the laser scanning setup is never used to its full mechanical capability. Conventional scanning speeds are around 2m.s^{-1} but the scan heads can mechanically move 10 to 20 times faster. This limitation avoids unwanted discontinuity of the local melting phenomenon on the powder bed. Consequently, linear descriptions of the mechanical parts of the actuator remain relevant since the standard operating conditions in actual machines continue to be subject to such scanning speed limitations. Therefore in the following, control techniques commonly applied to linear systems are used for the galvanometers.

Control structures are synthetized on the basis of a galvanometer model proposed in a previous work [11]. This model includes advanced torsion modes and friction models as illustrated in Figure 3. The input of the model is the voltage signal U and the angular position θ is the output. Its equivalent transfer function is denoted in the Figure 3 as $\boldsymbol{G_a}(s)$, s being the Laplace variable.

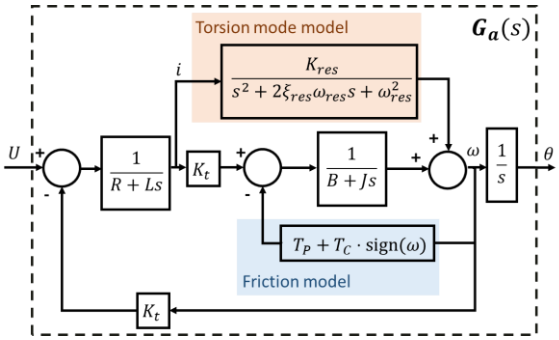

Figure 3. Galvanometer motor model.

The galvanometer parameters from Figure 3 are described in Table 1 with their numerical values for both axes:

Parameter [unit]	Description	x value	y value
R [Ohm]	Internal resistance	2.74	2.57
L [H]	Coiling inductance	2.24×10^{-4}	2.17×10^{-4}
K_t [V.s.rad^{-1}] or [N.m.A^{-1}]	Value of the back-EMF constant or the torque constant	9.3×10^{-5}	1.15×10^{-4}
B [N.m.s.rad^{-1}]	Viscous friction coefficient	10^{-9}	10^{-9}
J [kg.m^2]	Motor and load inertia	1.4×10^{-11}	1.53×10^{-11}
T_P [N.m] T_C [N.m]	Enhanced friction model parameters	3.13×10^{-6} 0.5×10^{-6}	4.15×10^{-6} 0.9×10^{-6}
K_{res} [rad.s^{-1}.A^{-1}] ξ_{res}[.] ω_{res} [rad.s^{-1}]	First resonance mode parameters of the motor-load link	0.002 0.005 5.31×10^4	0.0027 0.005 4.69×10^4

Table 1. Galvanometers x and y model parameters.

A first conventional PID-based control structure is implemented initially for each of the two axes (x and y) to replicate the commercial system behavior, which is considered as a black-box system. The chosen structure is presented in Figure 4.

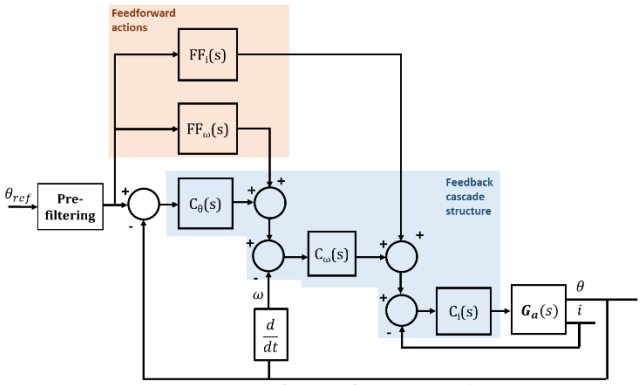

Figure 4. Conventional control structure of an axis.

The conventional structure consists of a three-loop feedback cascade controller: Proportional Integral controllers for the motor current and the motor rotation speed loops (respectively $C_i(s)$ and $C_\omega(s)$) and a Proportional Derivative controller ($C_\theta(s)$) for the angular position loop. Feedforward actions are introduced for the motor current and the motor rotation speed to optimize the system accuracy. The angular position reference θ_{ref} is limited in velocity, acceleration and jerk with a pre-filter. The filtering technique is based on the design of FIR (Finite Impulse Response) filters for planning minimum-time trajectories under speed, acceleration and jerk constraints as detailed in [12]. Tuning of the conventional control structure is achieved to provide a closed-loop bandwidth of 1.2 kHz for both galvanometers.

As a validation step, the positioning dynamics of the conventional control structure are compared, in the case of the x axis, to the commercial scanner system behavior. Figure 5 gives the angular responses to a velocity-limited multi-step reference which covers a maximum range of the angular capability of the galvanometer. The figure shows that the commercial system behavior can be reproduced in an accurate manner within the elaborated open-architecture test bench. The maximum angular difference between the commercial and the conventional structure responses is as small as 0.35deg, which is a reasonable value.

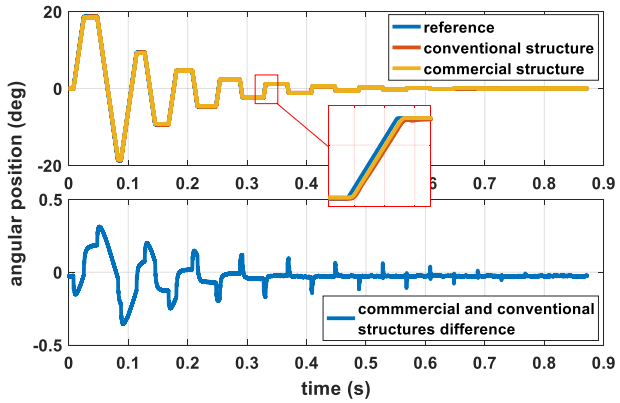

Figure 5. Experimental comparison of angular position responses of the commercial system and the conventional control structure and difference between these signals.

The H-infinity controller synthesis technique is presented below with its application to the galvanometers.

H-infinity controller synthesis

The main benefit of H-infinity controllers is the possibility to keep precision indicators degradation as low as possible while increasing system rapidity. As a matter of fact, H-infinity controller synthesis techniques allow simultaneous consideration of multiple control objectives which impact stability, rapidity and precision of the system.

H-infinity controller synthesis strategy [9] consists of the feedback controller $K(s)$ synthesis for a given system plant $P(s)$, as depicted in Figure 6 as the 'standard' form for the controller synthesis.

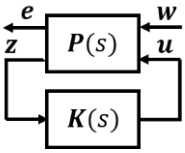

Figure 6. Standard problem form.

The closed-loop system can be rewritten as follows with the four transfer functions that constitute $P(s)$ between the reference input signals $\boldsymbol{w}$, the command signals $\boldsymbol{u}$, the monitored signals $\boldsymbol{e}$ and the measurements $\boldsymbol{z}$:

$$\begin{pmatrix}\boldsymbol{e}(s)\\ \boldsymbol{z}(s)\end{pmatrix} = P(s)\begin{pmatrix}\boldsymbol{w}(s)\\ \boldsymbol{u}(s)\end{pmatrix} = \begin{pmatrix}P_{\boldsymbol{ew}}(s) & P_{\boldsymbol{eu}}(s)\\ P_{\boldsymbol{zw}}(s) & P_{\boldsymbol{zu}}(s)\end{pmatrix}\begin{pmatrix}\boldsymbol{w}(s)\\ \boldsymbol{u}(s)\end{pmatrix} \quad (1)$$

The transfer function between $\boldsymbol{e}$ and $\boldsymbol{w}$ is as follows:

$$\begin{aligned}\boldsymbol{e}(s) &= \left(P_{\boldsymbol{ew}}(s) + P_{\boldsymbol{eu}}(s)K(s)\left(I - P_{\boldsymbol{zu}}(s)K(s)\right)^{-1}P_{\boldsymbol{zw}}(s)\right)\boldsymbol{w}(s)\\ &= \boldsymbol{F}_l\left(P(s), K(s)\right)\boldsymbol{w}(s)\end{aligned} \quad (2)$$

$\boldsymbol{F}_l\left(P(s), K(s)\right)$ is called the LFT (*Linear Fractional Transformation*) of the closed-loop system and the main objective of the H-infinity controller synthesis technique (also referred as the 'standard problem formulation') is defined for $P(s)$ and a given scalar γ and consists in finding $K(s)$ which stabilizes the closed-loop system while ensuring

$$\left\|\boldsymbol{F}_l\left(P(s), K(s)\right)\right\|_\infty < \gamma \quad (3)$$

The H-infinity (H_∞) norm $\|X(s)\|_\infty$ of a given system $X(s)$ is defined for a set of pulsations ω as:

$$\|X(s)\|_\infty := \sup_{\omega\in\mathbb{R}} \bar{\sigma}(X(j\omega)) \quad (4)$$

where $\bar{\sigma}$ depicts the highest singular value of the system. Consider a system $X(s)$ represented as a transfer functions matrix, with p and m as the respective dimensions of the input and the output vectors. The singular values $\bar{\sigma}_i$ for $i = 1$ to $\min(p, m)$ are defined as the square roots of the eigenvalues λ_i of the multiplication of the transfer matrix with its conjugate transpose:

$$\sigma_i(X(j\omega)) := \sqrt{\lambda_i(X(j\omega)X(-j\omega)^T)} \quad (5)$$

For the univariate case, the H-infinity norm depicts the highest values of the system gain module. The H-infinity controller synthesis technique consists mainly in shaping the gain modules of the LFT, therefore the gain modules of the four transfer functions of $P(s)$ as seen in the expression (2).

To find a solution to the standard problem, hence γ and $K(s)$, the Glover-Doyle algorithm [13] is the most commonly used method. It is sometimes referred to as the 'Riccati equations method'. A state-space representation of $P(s)$ is derived from (1) such as:

$$\begin{pmatrix}\dot{x}(t)\\ e(t)\\ z(t)\end{pmatrix} = \begin{pmatrix}A & B_w & B_u\\ C_e & D_{ew} & D_{eu}\\ C_z & D_{zw} & D_{zu}\end{pmatrix}\begin{pmatrix}x(t)\\ w(t)\\ u(t)\end{pmatrix} \quad (6)$$

with $x \in \mathbb{R}^n, w \in \mathbb{R}^{nw}, u \in \mathbb{R}^{nu}, e \in \mathbb{R}^{ne}, z \in \mathbb{R}^{nz}$

Let $P = P^T$ ($\cdot^T$ notation is for matrix transpose) and $Q = Q^T$ be two matrices with the same dimension as A from (6) and

$$X = Ric\begin{pmatrix}A & -P\\ -Q & -A^T\end{pmatrix} \quad (7)$$

the solution to the Riccati equation:

$$XA + A^TX - X^TPX + Q = 0 \quad (8)$$

such that all eigenvalues of $A - PX$ have a strictly negative real part.

The feasibility of the standard problem is defined by the following five conditions:

i. $H_\infty = \begin{pmatrix}A & \gamma^{-2}B_wB_w^T - B_uB_u^T\\ -C_e^TC_e & -A^T\end{pmatrix}$ does not have any imaginary eigenvalue
ii. There exists a matrix $X_\infty = Ric(H_\infty)$, a definite positive matrix (a matrix which has only positive eigenvalues)
iii. $J_\infty = \begin{pmatrix}A^T & \gamma^{-2}C_e^TC_e - C_z^TC_z\\ -B_wB_w^T & -A\end{pmatrix}$ does not have any imaginary eigenvalue
iv. There exists a matrix $Y_\infty = Ric(J_\infty)$, a definite positive matrix
v. $\rho(X_\infty Y_\infty) < \gamma^2$ where $\rho(X_\infty Y_\infty)$ depicts the module of the highest eigenvalue of the matrix $X_\infty Y_\infty$

Under these feasibility conditions, the solution to the standard problem gives the controller $K(s)$ stabilizing $P(s)$ and fulfilling (3) such as:

$$K(s) = \boldsymbol{F}_l(K_a(s), \Phi(s)) \tag{9}$$

where $\Phi(s)$ is an arbitrary transfer functions matrix of $nu \times nz$ dimension and of H_∞ norm lower than γ and $K_a(s)$ is represented in the state-space form:

$$\begin{pmatrix} \dot{x}_a(t) \\ u(t) \\ u_a(t) \end{pmatrix} = \begin{pmatrix} \hat{A}_\infty & Z_\infty Y_\infty C_z^T & Z_\infty B_u \\ -B_u^T X_\infty & 0 & I_{nu} \\ -C_z & I_{nz} & 0 \end{pmatrix} \begin{pmatrix} x_a(t) \\ z(t) \\ z_a(t) \end{pmatrix} \tag{10}$$

where

$\hat{A}_\infty = A + \gamma^{-2} B_w B_w^T X_\infty - B_u B_u^T X_\infty - Z_\infty Y_\infty C_z^T C_z$

$Z_\infty = (I_n - \gamma^{-2} Y_\infty X_\infty)^{-1}$

I_n is the identity matrix of dimension n

The 'central controller' is defined for the particular case $\Phi(s) \equiv 0$ which state-space representation is as follows:

$$\begin{pmatrix} \dot{x}_c(t) \\ u(t) \end{pmatrix} = \begin{pmatrix} \hat{A}_\infty & Z_\infty Y_\infty C_z^T \\ -B_u^T X_\infty & 0 \end{pmatrix} \begin{pmatrix} x_c(t) \\ z(t) \end{pmatrix} \tag{11}$$

The resolution of the standard problem uses the five feasibility conditions i to v to approach the optimal value of γ by dichotomy. The central controller is computed thereafter from the equations (9) to (11).

The H-infinity controller synthesis technique has to be applied to a chosen synthesis model which is selected in the galvanometer case as the galvanometer system along with the current controller in order to keep the current response dynamics of the conventional structure. The resulting synthesis model $\boldsymbol{G}(s)$ is presented in Figure 7. The friction model has been intentionally omitted due to the discontinuity aspect of the 'sign' function.

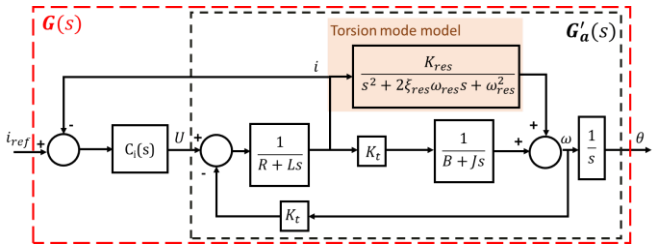

Figure 7. Galvanometer model with current controller considered for the H-infinity synthesis technique.

It is common to apply weighting filters on the signals of the resulting closed-loop system in the scope of the H-infinity controller synthesis technique [9] in order to allow for additional tuning parameters for the procedure. These filters are applied to the signals of the resulting closed-loop system. Three filters are usually introduced for the error difference signal ($\varepsilon = \theta_{ref} - \theta$), the command signal ($u = i_{ref}$ in the galvanometer case) and an additional disturbance entry b considered on the command signal. The resulting system plant $P(s)$ for the standard form along with the weighting filters is illustrated in Figure 8.

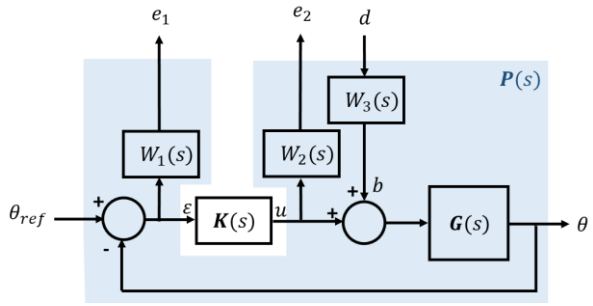

Figure 8. Closed-loop structure for the H-infinity synthesis technique.

The disturbance signal b on the command signal is considered as the output of the filter $W_3(s)$ which has an input signal d. ε and u are the inputs of the $W_1(s)$ and $W_2(s)$ filters respectively. The weighting filters are chosen to be first order filters to minimize the complexity of the resulting plant $P(s)$. The parametrization of these filters is as follows:

$$W_j(s) = \left(\frac{a_j s + b_j}{c_j s + d_j}\right)^{-1} \tag{12}$$

The four parameters of each filter are chosen according to the corresponding closed-loop transfer functions that are impacted. These transfer functions are introduced below.

With the new form of $P(s)$ from Figure 8, the derived output vector can be written as $\boldsymbol{e} = \begin{pmatrix} e_1 \\ e_2 \end{pmatrix}$, the input as $\boldsymbol{w} = \begin{pmatrix} \theta_{ref} \\ d \end{pmatrix}$ and the resulting LFT for the standard form is as:

$$\begin{cases} \boldsymbol{F}_l\big(P(s), K(s)\big) := \begin{pmatrix} W_1(s)S(s) & -W_1(s)S(s)G(s)W_3(s) \\ W_2(s)K(s)S(s) & -W_2(s)T(s)W_3(s) \end{pmatrix} \\ S(s) = \big(1 + G(s)K(s)\big)^{-1} \\ T(s) = 1 - S(s) \end{cases} \tag{13}$$

The inequality (3) then becomes:

$$\left\| \begin{matrix} W_1(s)S(s) & -W_1(s)S(s)G(s)W_3(s) \\ W_2(s)K(s)S(s) & -W_2(s)T(s)W_3(s) \end{matrix} \right\|_\infty < \gamma \tag{14}$$

A property of the H-infinity norm [9] states that if the H-infinity norm of a transfer function matrix admits an upper bound, all of its elements admit the same bound. (14) is therefore equivalent to:

$$\begin{cases} \|W_1(s)S(s)\|_\infty < \gamma \Leftrightarrow \forall \omega \in \mathbf{R}\, |S(j\omega)| < \frac{\gamma}{|W_1(j\omega)|} \\ \|W_2(s)K(s)S(s)\|_\infty < \gamma \Leftrightarrow \forall \omega \in \mathbf{R}\, |K(j\omega)S(j\omega)| < \frac{\gamma}{|W_2(j\omega)|} \\ \|W_1(s)S(s)G(s)W_3(s)\|_\infty < \gamma \Leftrightarrow \forall \omega \in \mathbf{R}\, |S(j\omega)G(j\omega)| < \frac{\gamma}{|W_1(j\omega)W_3(j\omega)|} \\ \|W_2(s)T(s)W_3(s)\|_\infty < \gamma \Leftrightarrow \forall \omega \in \mathbf{R}\, |T(j\omega)| < \frac{\gamma}{|W_2(j\omega)W_3(j\omega)|} \end{cases} \tag{15}$$

The inequalities (15) explicitly show that the transfer functions $S(s)$, $K(s)S(s)$, $S(s)G(s)$ and $T(s)$ of the resulting closed-loop system can be adjusted by means of parametrization of the weighting filters $W_1(s)$, $W_2(s)$ and $W_3(s)$, thus the choice of the four parameters a_j, b_j, c_j and d_j in (12) for each filter. $W_1(s)$ is the most important of the three filters, because it allows for adjusting the rapidity (bandwidth), the precision and the stability of the resulting closed-loop system. Additionally, the tuning of $W_2(s)$ and $W_3(s)$ allows for adjusting high frequency noise rejection and robustness to neglected system dynamics. As an illustration, the

filters' parameters used for both axes x and y are given in Table below. The parameters are chosen in order to reproduce the rapidity of the conventional control structure with a closed-loop bandwidth of 1.2 kHz.

Parameter	Value
a_1	1.001
b_1	0.1342
c_1	1
d_1	134.2
a_2	5.499
b_2	2.463×10^7
c_2	54.99
d_2	4.477×10^5
a_3	13.47
b_3	1962
c_3	14.97
d_3	130.8

Table 2. Weighting filters parameters values for H-infinity controller synthesis.

Once the weighting filters are chosen, the corresponding H-infinity controller $K(s)$ is computed by the aforementioned Glover-Doyle algorithm.

In the same way that the current controller has been retained from the conventional control structure, the feedforward action for the current is also maintained in the final galvanometer axis structure in order to keep the achieved precision. The resulting structure of a single axis of the 2-axis scanner system is depicted in Figure 9 where $K(s)$ is the H-infinity controller computed with the Glover-Doyle algorithm.

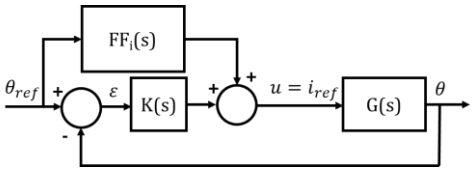

Figure 9. Axis control structure with H-infinity controller.

The H-infinity controller axis control structure is compared first in terms of frequency responses to the conventional structure of Figure 4. For illustration purposes, the closed-loop angular position $\frac{\theta}{\theta_{ref}}$ response and the sensitivity function S (as defined in (13)) are compared in Figure 10 for the x axis galvanometer.

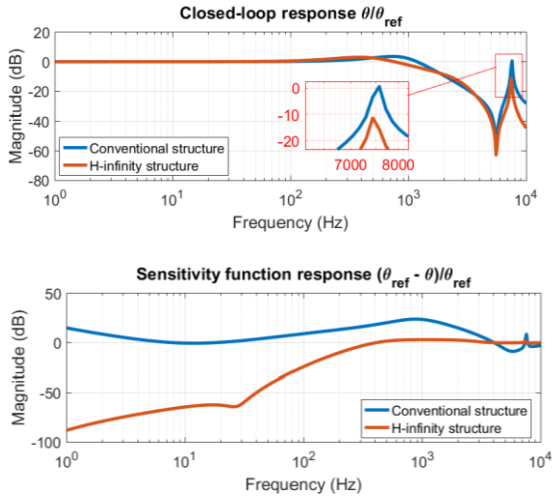

Figure 10. Frequency responses comparison between conventional and H-infinity controller structures.

The following numerical values are derived from Figure 10, their meanings are described shortly after Table 3:

Performance indicators	Conventional structure	H-infinity structure
Bandwidth*	1.2kHz	1.2kHz
First resonance attenuation**	0.65dB	-11.22dB
Sensitivity function maximum magnitude***	23.91dB	3.09dB

Table 3. Frequency responses parameters comparison between conventional and H-infinity controller structures.

* The bandwidth of the closed-loop system defines its rapidity, this parameter is tuned to be of the same value for the two structures for comparison purposes

** The first resonance attenuation in the closed-loop frequency response impacts the stability of the system, it should be as low as possible

*** The maximum value of the sensitivity function also impacts the stability of the system and should be as low as possible

As a second comparison, the angular responses of the two controller structures to an angular step from -2deg to +2deg are presented in Figure 11 for the x axis galvanometer:

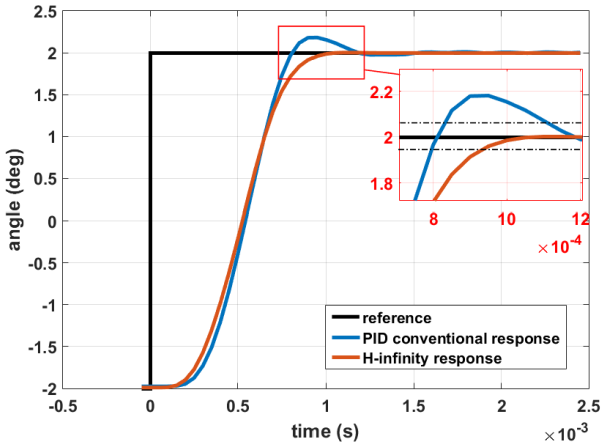

Figure 11. Time responses comparison of the controller structures to a step signal.

Angular responses characteristics from Figure 11 are given in the Table 4 below:

Response characteristics	Conventional structure	H-infinity structure
Settling time to 2% error from final value	11ms	9.5ms
Maximum overshoot	4.53%	0%

Table 4. Step responses characteristics comparison

The most significant result from Table 4 is the maximum overshoot of the responses which is eliminated for the H-infinity structure, meaning that the closed-loop response in this case is more stable than that of the conventional control structure. The settling time to 2% error from the final value is also 0.15ms smaller for the H-infinity structure, the angular positioning rapidity is therefore improved.

As a final illustration for the positioning performance achieved with the H-infinity controller, the experimental time domain responses to the multi-step reference input of Figure 5 are

compared for the two structures in terms of the error difference between the reference signal and the responses. Results are presented in Figure 12.

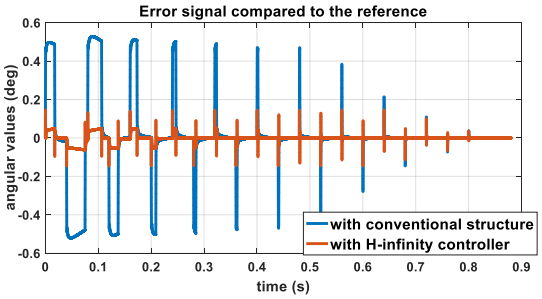

Figure 12. Experimental error signals comparison for the velocity-limited multi-step reference.

It is shown that the error difference signal values are mostly smaller in the case of the H-infinity controller structure. Maximum error signal values go up to 0.5deg for the conventional structure while it does not exceed 0.15deg for the H-infinity structure.

Achievable precision improvement with the H-infinity controller structure is presented below in the context of an experimental SLM job example with optimized scanning speed.

Results on a marking job with optimized scanning speed on the 2-axis experimental test bench

A SLM marking job is performed with different operation speed settings on the open architecture test bench in the case of axes driven by the conventional and the H-infinity control structures. The job consists in the realization of 100 cubes whose side length is equal to 10mm as illustrated in Figure 13.

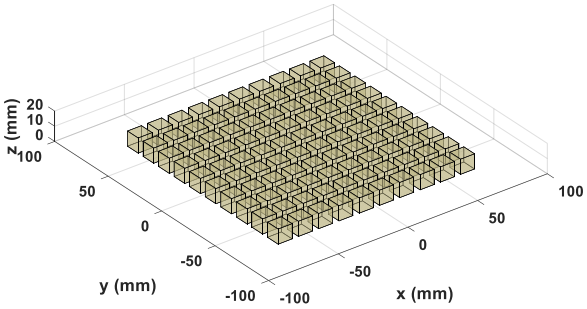

Figure 13. SLM job of 100 cubes.

Results are given for the realization of a single cross-section (layer) of the job in the (x, y) plane, the z dimension can be taken into account with the value of the layer thickness of the SLM operation.

Work plane values (x, y) and galvanometer angular values (θ_x, θ_y) are related by means of the so-called 'Geometrical models' of the 2-axis system. The simplest expression of those models [14] are deployed in this work for illustration purposes in the (x, y) coordinates. The parametrization of the 2-axis system for the geometrical models expression is presented in Figure 14.

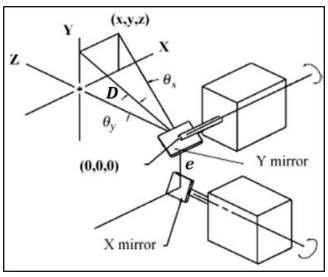

Figure 14. Parametrization of the 2-axis scanning system [15]

The expressions of the direct and the inverse models, respectively, which derive from Figure 14, are given as follows:

$$\begin{cases} x = \left(\frac{D}{\cos(2\theta_y)} + e\right)\tan(2\theta_x) \\ y = D\tan(2\theta_y) \end{cases} \quad (16)$$

$$\begin{cases} \theta_x = \frac{1}{2}\tan^{-1}\left(\frac{x}{\sqrt{y^2+D^2}+e}\right) \\ \theta_y = \frac{1}{2}\tan^{-1}\left(\frac{y}{D}\right) \end{cases} \quad (17)$$

e is the distance between the two mirrors and D is the distance between the second galvanometer mirror and the marking plane.

As stated earlier, marking results are given for a single layer cross-section of the original job of Figure 13. Therefore, cubes marking is equivalent to filled squares marking. A traditional technique to mark a filled square is presented in Figure 15.

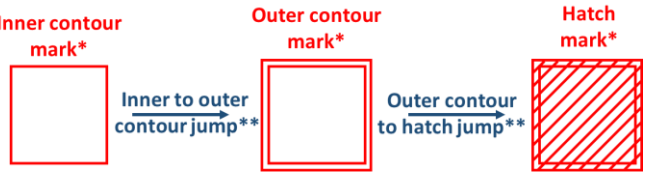

Figure 15. Scanning sequence at the single square level.

The scanning sequence of the filled square consists in two concentric contour and a 45degree-oriented hatch pattern.

* mark operations are defined when laser power is 'on'

** jump operations are defined when laser power is 'off'

The scanning sequence at the layer level is presented in Figure 16. The first square to mark is at the bottom right of the work plane and the last one is at the top left. Jump operations as illustrated in Figure 16 are executed when going from a filled square to another.

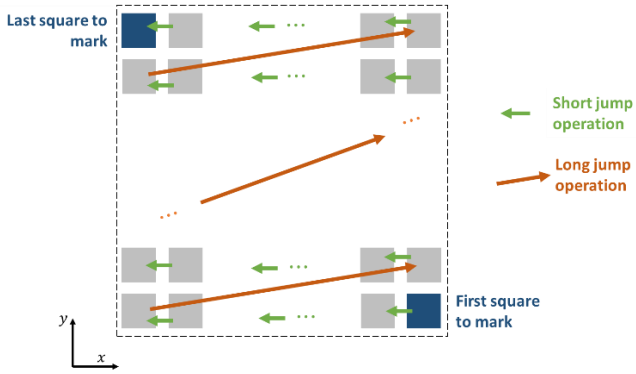

Figure 16. Scanning sequence at the layer level.

Two sets of scanning speed parameters are considered and implemented on the open architecture 2-axis test bench:

- A 'default' setting of scanning speeds issued from an industrial scanning head:
  - Contours marking speed: 1500mm/s
  - Hatch marking speed: 1000mm/s
  - Inner to outer contour jump: 4500mm/s
  - Outer contour to hatch, short and long jumps: 6000mm/s

- A 'harmonized' setting of scanning speeds adjusted to optimize the overall scanning speed therefore the scanning operation duration:
  - All mark operations: 1500mm/s
  - All jump operations: 6000mm/s

The operation speed harmonization is proposed in order to measure the time gain achievement along with the precision performance between the two scanning speed settings for the two types of galvanometers control structure: conventional and H-infinity.

Marking operation precision is quantified in comparison with the desired filled squares (references) in terms of contouring error for the contours marking and of a defined filling ratio for the hatch pattern marking. Contouring error, defined as the smallest distance at each point of the actual trajectory to the reference trajectory is illustrated in Figure 17. The 'linear interpolation' method in [16] is used for the results that will be presented.

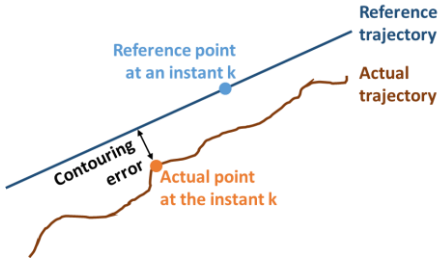

Figure 17. Contouring error illustration.

The desired filled square surface is discretized into smaller squares with side length equal to the laser spot diameter (chosen by default from the industrial scanning head to 70µm). A small discrete square is tagged 'filled' when the laser trajectory has got points located inside of it. The filling ratio for hatch marking is illustrated in Figure 18 and is defined as the ratio between the number of filled discrete squares and the total number of discrete squares for the desired surface.

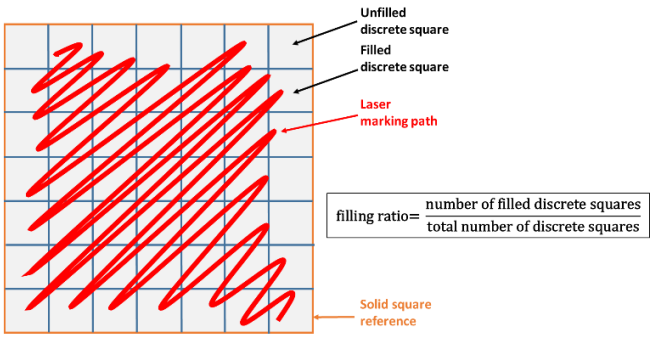

Figure 18. Filling ratio illustration.

The two scanning speed settings are implemented experimentally on the open architecture test-bench for axes with conventional and H-infinity control structures. For a single layer of the marking job, for the default speed settings, measured operation duration is 118.014 seconds whereas for the harmonized setting it is 87.714 seconds. There is consequently a 26% gain in terms of operation time. For precision performance, results are summarized in the following Table 5 where contouring errors and filling ratios are presented. For the contouring errors, three thresholds of precision values are given to illustrate the evolution of the results. The values of the table correspond to the proportion of laser trajectory points on the entire job that achieve contouring error values fulfilling the given conditions.

		Default speed setting		Harmonized speed setting	
		Conventional control	H-infinity control	Conventional control	H-infinity control
Contouring error	<100µm	37.85%	85.65%	47.56%	84.2%
	<200µm	90.55%	95.68%	91.9%	94.35%
	<300µm	96.59%	98.33%	96.9%	96.97%
Filling ratio		68.47%	70.11%	54.28%	56.41%
Operation duration		118.014 seconds		87.714 seconds	

Table 5. Marking job precision performance summary.

The overall resulting filling ratio values are relatively low and can be improved by choosing the laser spot diameter value according to the test bench parameters (the sampling period value in the dSpace interface board in particular). The default laser spot diameter value of 70μm corresponding to the Table 5 results can be increased, however, these results are given for a relative comparison between the experimental results of the two control structures.

It is shown in Table 5 that precision performance for axes driven by H-infinity controller structure is always greater than the performance of axes with conventional control structures. The precision of contour marking is highly improved for example in terms of the proportion of trajectory points that present a contouring error less than 100µm. Both structures minimize performance loss from the first speed settings to the second. In terms of filling ratio, the performance achieved with H-infinity control structures remains greater by about 2%.

Conclusions

This paper presented the achievable benefits of an H-infinity controller structure for the control of the galvanometer motor, which is the main actuator of SLM machines for AM. In comparison to conventional PID-based control, results obtained on an open architecture experimental test bench show that this advanced controller increases the system precision performance while operation speed is optimized. Additive manufacturing 'Key Performance Indicators' (KPI) such as part porosity and melt pool characteristics depend mostly on one main process parameter: the scanning speed [17] whilst operation precision is often neglected. The study carried out in this paper emphasizes the combined effect of operation rapidity and precision on KPIs.

To illustrate this, three indicators are defined from Table 5:

- a *precision indicator* with a value in [0, 1] : which is the mean value of the four percentage values from each column of Table 5
- a *scanning time indicator* with a value in [1, +∞[: which is calculated by dividing the maximum recorded scanning

time on all the trials (here equals to 118.014seconds) by the current scanning time

- an *overall indicator* with a value in [0, +∞[and calculated with the formula:

$$overall\ indicator = \alpha \cdot precision\ indicator + (1 - \alpha) \cdot scanning\ time\ indicator$$

α is chosen in [0, 1] as a weighting factor for putting focus whether on the precision or the scanning time indicator (in particular, $\alpha = 0.5$ puts the same weight on both). Results are presented in Figure 19.

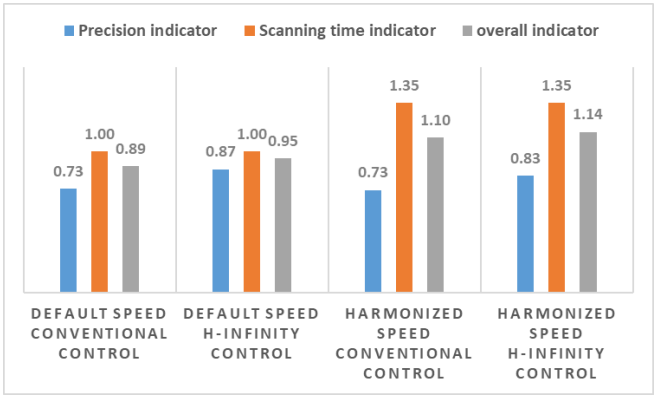

Figure 19. Process parameters performance indicators.

Higher values of the indicators means higher performance of the positioning system thus higher impacts on KPIs. Figure 19 shows the combined impact of the precision and scanning time indicators and the quantification of the performance enhancement achieved with the H-infinity control structure.

Further research perspectives might consider the thermal aspect of SLM operation in order to investigate the influence of the optimized speed settings on the laser spot shape and the local melting pool on the powder bed, which has a major impact on the mechanical properties of the final part.

Acknowledgments

This work takes part in the SOFIA project context. SOFIA is an applied research program for metal additive manufacturing, initiated by AddUp, a Fives & Michelin Joint Venture dedicated to Additive manufacturing solutions. SOFIA is funded by the Auvergne Rhone-Alpes region as well as Bpifrance as a structuring R&D project for competitiveness, within the 'Investing for the Future' program.

References

[1] Schmidt M, Merklein M, Bourell D, Dimitrov D, Hausotte T, Wegener K, Overmeyer L, Vollertsen F, Levy GN (2017) Laser Based Additive Manufacturing in Industry and Academia. *CIRP Annals* 66(2):561–583.

[2] Schmid M, Levy G (2012) Quality management and estimation of quality costs for Additive Manufacturing with SLS. *Fraunhofer Direct Digital Direct Manufacturing Conference.*

[3] Bikas, H., Stavropoulos, P., & Chryssolouris, G. (2016). Additive manufacturing methods and modelling approaches: a critical review. *The International Journal of Advanced Manufacturing Technology*, 83(1-4), 389-405.

[4] Aylward, RP (2003). Advanced galvanometer-based optical scanner design. *Sensor review* 23(3):216-222.

[5] Iwasaki M, Seki K, Maeda Y (2012). High-precision motion control techniques: A promising approach to improving motion performance. *IEEE Industrial Electronics Magazine* 6(1): 32-40.

[6] Hirose N, Iwasaki M, Kawafuku M, Hirai H (2009). Initial value compensation using additional input for semi-closed control systems. *IEEE Transactions on Industrial Electronics*. 56(3):635-641.

[7] Kim BK, Chung WK, Ohba K (2009). Design and performance tuning of sliding-mode controller for high-speed and high-accuracy positioning systems in disturbance observer framework. *IEEE Transactions on Industrial Electronics*. 56(10):3798-3809.

[8] Zaeh M, Pieczona S J (2018). Adaptive inverse control of a galvanometer scanner considering the structural dynamic behavior. *CIRP Annals* 67(1):385-388.

[9] Zhou K, Doyle JC, Glover K (1996). *Robust and optimal control*. Prentice hall, New Jersey.

[10] Kaur, R., & Ohri, J. (2014). H-infinity controller design for pneumatic servosystem:a comparative study. *International Journal of Automation and Control*, 8(3), 242-259.

[11] Rasoanarivo F, Rodriguez-Ayerbe P, Dumur D (2018) Galvanometer scanner modeling for Selective Laser Melting Deflection system simulation. *15th International Conference on Control, Automation, Robotics and Vision (ICARCV)*:1170-1175.

[12] Biagiotti L, Melchiorri C (2012). FIR filters for online trajectory planning with time-and frequency-domain specifications. *Control Engineering Practice*, 20(12): 1385-1399.

[13] Doyle, J. C., Glover, K., Khargonekar, P., & Francis, P. (1989). 'State Space Solutions to Standard H-2 and H-infinity. *IEEE Trans. Autom. Control, AC*, 34, 831-847.

[14] Xie, J., Huang, S., Duan, Z., Shi, Y., & Wen, S. (2005). Correction of the image distortion for laser galvanometric scanning system. *Optics & Laser Technology*, 37(4), 305-311.

[15] Nee, A., J. Fuh et T. Miyazawa. 2001, «On the improvement of the stereolithography (sl) process», Journal ofMaterials Processing Technology, vol. 113, no 1-3, p. 262–268.

[16] Duong, T. Q., Rodriguez-Ayerbe, P., Lavernhe, S., Tournier, C., & Dumur, D. (2016, July). Offline gain adjustment with constraints for contour error reduction in high speed milling. In *2016 IEEE International Conference on Advanced Intelligent Mechatronics (AIM)* (pp. 201-206). IEEE.

[17] Stavropoulos, P., & Foteinopoulos, P. (2018). Modelling of additive manufacturing processes: a review and classification. *Manufacturing Review*, 5, 2.